Catalysis Today 169 (2011) 232–241

Contents lists available at ScienceDirect

Catalysis Today

journal homepage: www.elsevier.com/locate/cattod

Toward redox framework single site zeolite catalysts

Stanislaw Dzwigaj[a,b,*], Michel Che[a,b,c]

[a] Laboratoire de Réactivité de Surface, UPMC Univ Paris 6, 4 Place Jussieu, 75252 Paris Cedex 05, France
[b] Laboratoire de Réactivité de Surface, CNRS, UMR 7197, 4 Place Jussieu, 75252 Paris Cedex 05, France
[c] Institut Universitaire de France, France

ARTICLE INFO

Article history:
Received 9 August 2010
Received in revised form 11 January 2011
Accepted 18 January 2011
Available online 25 February 2011

This paper is dedicated to the memory of the late Professor Jerzy Haber, a great scientist and an outstanding lecturer.

Keywords:
Redox
Framework
Single site
BEA
Catalyst
Transition element

ABSTRACT

This paper concerns heterogeneous single site catalysts which are difficult to prepare because of speciation problems related to the two starting components, the solid and the metal precursor solution. A two-step post-synthesis method is used to prepare the V–SiBEA reference system, with vanadium in framework position. In the light of the molecular processes identified for each step of the post-synthesis method, other transition elements are selected and investigated. The pros and cons of the method are discussed. While *redox* zeolites with *isolated* and *framework* metal centres have been successfully obtained, the results raise the question as to which extent the latter have to be *identical*, from a chemical and/or topological point of view.

1. Introduction

It has been a great experience to witness Jerzy Haber's career developing over more than 50 years and to learn so much from his vision of catalysis, expressed in his numerous publications and fascinating lectures. Looking at his 100 most cited papers (obtained from the web of knowledge site), one can see that the large majority (about 83) concerns transition metal oxides, the rest being shared between heteropolyacids (12) and zeolites (5). The reason for the large predominance of transition metal oxides is to be found in their decisive role in the selective oxidation of hydrocarbons, particularly vanadium oxide catalysts that Jerzy investigated so insightfully both experimentally and theoretically. With the recoil, the last sentence of his review "Fifty years of my romance with vanadium oxide catalysts" is particularly moving to read: "On the basis of the results collected in the last 50 years, a book on physical chemistry of vanadium–oxygen system could be written" [1]. It is a real pity that Jerzy will never write this book.

With the present contribution, we would like to pay a tribute to Jerzy and our long-lasting friendship and collaboration [2–12], by adding yet another chapter on vanadium oxide catalysts but investigated this time from the angle of molecular catalysts. The challenge was to prepare *redox single site* zeolite catalysts with transition metal atoms in *framework* position.

2. Actives sites: the lesson of Taylor

On the basis of poisoning experiments performed with CS_2 by French workers on platinum black catalyst of the hydrogenation of propylketone, piperonal and nitrobenzene [13], Taylor came up with several important conclusions in his famous paper entitled "A theory of the catalytic surface" [14]. In connection with our paper, we wish to emphasize the one related to active sites: "...the amount of surface which is catalytically active is determined by the reaction catalyzed. There will be all extremes between the cases in which all the atoms of the surface are active and that in which relatively few are so active". Although Taylor referred mainly to metal surfaces, the same reasoning can be extended to catalytic systems where the active phase (a transition metal oxide or a metal) is supported on an oxide. In such systems, e.g., VO_x/Al_2O_3 or Pt/SiO_2, the catalytically active element, hereafter referred to as metal centre, is V or Pt respectively.

---

* Corresponding author at: Laboratoire de Réactivité de Surface, UPMC Univ Paris 6, 4 Place Jussieu, 75252 Paris Cedex 05, France.
E-mail address: stanislaw.dzwigaj@upmc.fr (S. Dzwigaj).

0920-5861/$ – see front matter © 2011 Elsevier B.V. All rights reserved.
doi:10.1016/j.cattod.2011.01.035

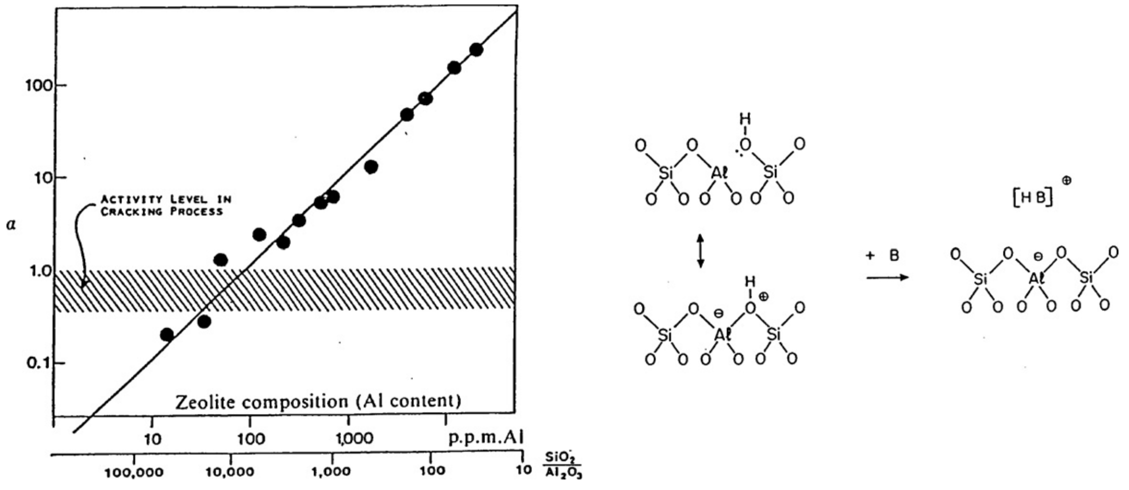

Fig. 1. Hexane cracking activity α plotted against the aluminium content in HZSM-5 and nature of the corresponding active site, according to Ref. [20].

3. Single site catalysts: the goal

Taking further the conclusion of Taylor quoted above, Boudart [15] distinguished two extreme cases: one in which all surface metal centres are active but possess different activities and the other where *all* the metal centres are active and exhibit the *same* activity. The latter case corresponds to molecular catalysts or single site catalysts. The term single site was used for the first time quickly after it was discovered that catalysts constituted by zirconocene complexes associated with methylalumoxane (MAO) exhibited unprecedented activity and selectivity in olefin polymerization [16,17]. Both homogeneous [18] and heterogeneous [19] single site olefin polymerization catalysts have since been reviewed.

For non polymerization catalysts, the best documented example of heterogeneous single site catalyst, according to Boudart [15], is illustrated by zeolites such as H-ZSM-5 (MFI) investigated in the cracking of n-hexane by Haag et al. [20]. By contrast with zeolites such as X and Y used as acid catalysts, the aluminium atom concentration in ZSM-5 is sufficiently low to be representative of a *dilute* solution. It can nevertheless be varied over several orders of magnitude (from *ca.* 20 to a few 10,000 ppm). The active sites were identified to be the tetrahedral Al atoms and their associated protons present in the zeolite (Fig. 1) and Haag et al. showed that there was a complete proportionality of activity and number of Al atoms, consistent with the homogeneity of the active sites from which absolute turnover rates and numbers were obtained, resembling the enzymatic turnover numbers.

We now wish to describe the problems involved in the preparation of heterogeneous single site catalysts.

4. Heterogeneous single site catalysts and speciation: two conflicting views

In the case of supported systems, generally prepared by impregnation of an oxide support by an aqueous solution of a precursor of the catalytically active phase, the obtention of single site catalysts is most difficult. The difficulty resides in the so-called speciation, which is "the distribution of an element amongst defined chemical species in a given system" [21], where chemical species are "the specific form of an element defined as to isotopic composition, electronic or oxidation state, and/or complex or molecular structure". Speciation concerns both the aqueous solution and the oxide support.

Fig. 2 gives for example the speciation of uranium(VI) in an aqueous environmental medium [22]. This diagram shows that, for a given uranium concentration, several types of complexes generally coexist.

The same holds true for the speciation of oxygen at the surface of an oxide. Depending on the experimental conditions, the surface of say MgO, with the simple rock salt (NaCl) structure (each ion in the bulk is sixfold coordinated), exhibits a complex distribution of surface hydroxyl groups and oxide ions. Even if surface hydroxyl groups have been carefully removed by high temperature outgassing, and in the absence of adsorbed molecular oxygen species [23], the speciation of oxygen remains complex with various concentrations of oxide ions in positions of low coordination (LC) $O^{2-}{}_{LC}$, with LC = 5C, 4C, 3C for an oxide ion on a face, edge or corner respectively (Fig. 3) [24].

The problem arises as to how single site catalysts with all *identical* and *well separated* active sites may be designed in view of the two types of complexity described above, one arising from the precursor aqueous solution, the other from the oxide support.

We first have tried to avoid the complexity of oxide supports by selecting zeolite systems. As a matter of fact, with such materials we move from solids with a number, generally undetermined, of active sites exposed on the oxide surface to an essentially "transparent solid solvent" where all intra-crystalline sites can interact

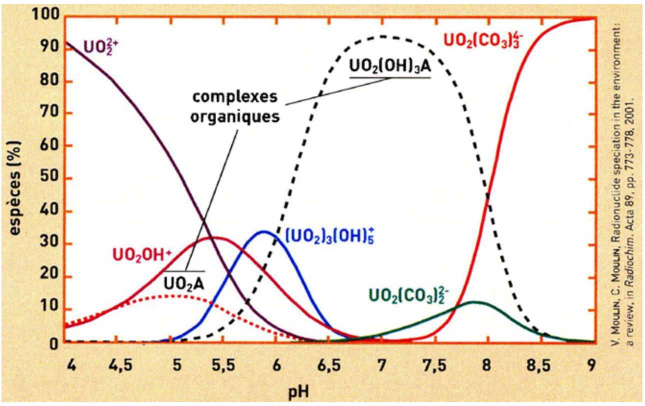

V. Moulin, C. Moulin, Radionuclide speciation in the environment: a review, in *Radiochim. Acta* 89, pp. 773-778, 2001.

Fig. 2. Speciation diagram of uranium(VI) in environmental medium in the presence of natural organic matter (humic substances A) with uranium concentration [U] = 1 mg/L, humic compounds [A] = 1 mg/L, non complexing medium of $NaClO_4$ of ionic strength 0.1 M, partial pressure of CO_2 [pCO_2] of 10–3.5 atm, according to Ref. [22].

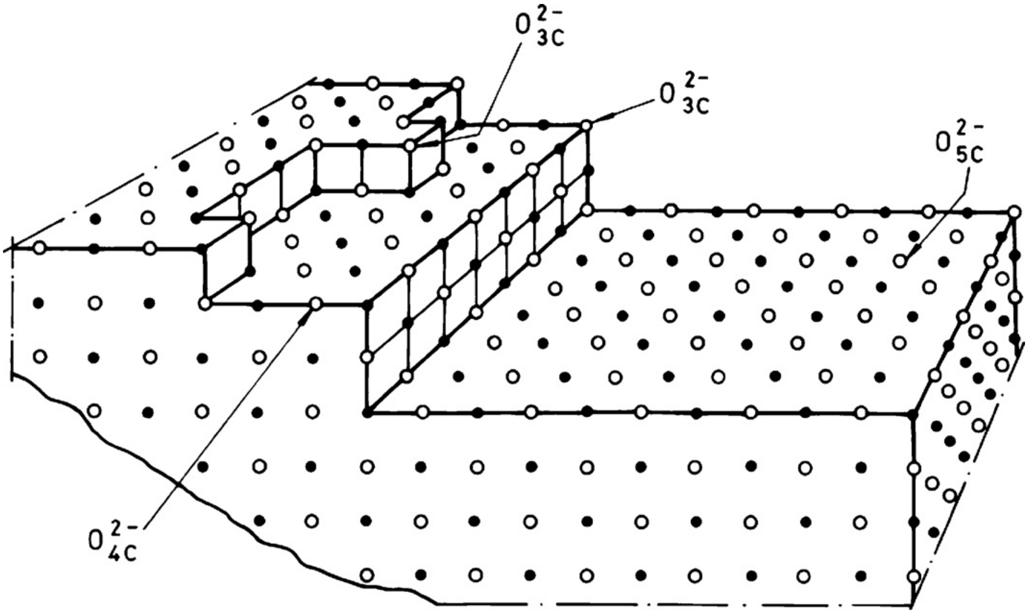

Fig. 3. Representation of a surface (0 0 1) plane of MgO, according to Ref. [24], which illustrates the speciation of oxygen. Black circles represent Mg^{2+-} ions and white circles oxide O^{2-} ions. Surface imperfections such as steps, kinks and corners provide sites for oxide ions in positions of low coordination $O^{2-}{}_{LC}$, with LC = 5C, 4C, 3C (see text).

with gas or liquid phase molecules. In order to have aluminium atoms sufficiently diluted in the zeolite matrix, high silica zeolites (with Si/Al ratio typically above *ca.* 10) such as ZSM-5 or BEA have to be preferred. For Si/Al ratios greater than 2, the distribution of aluminium atoms should approach randomness [25], with relative distance equivalent to several to many atomic diameters.

Apart from its high Si/Al ratio (typically above *ca.* 10), zeolite BEA, first prepared in 1967 at the Mobil Research and Development Laboratories [26], was selected for the following reasons: (i) it has a three-dimensional structure, (ii) it possesses pores larger than those of ZSM-5 with 12-membered ring openings (0.75 by 0.57 nm for linear and 0.65 by 0.56 nm for tortuous channels), (iii) it exhibits high thermal and acid stability [27].

5. Strategy toward redox framework single site zeolite catalysts: the two-step post-synthesis method applied to vanadium–BEA zeolites and the associated molecular processes

In order to *incorporate* metal atoms into the zeolite framework, we have developed a post-synthesis method, first applied to obtain vanadium–BEA zeolites (V_xSiBEA, with *x* being the vanadium wt.%). The preparation involves two successive steps [28], as illustrated by Fig. 4:

(i) removal of aluminium atoms from the framework upon treatment of BEA zeolite at 353 K for 4 h by a 13 N nitric acid solution, as described earlier [29] and
(ii) incorporation of vanadium at room temperature and atmospheric pressure, from an aqueous NH_4VO_3 solution, into the vacant sites created by the departure of aluminium in the first step.

The choice of the experimental conditions was governed by the fact that the metal atoms to be incorporated into the framework have to be, like the removed aluminium atoms, positively charged and mononuclear. The predominance diagram of vanadium(V) [30] (Fig. 5) shows that the only suitable species is $VO_2{}^+$ limiting the domain to low molality and pH.

The molecular processes associated with each of the two steps have been investigated both at the macroscopic and at the molecular levels by means of appropriate techniques before the solids obtained were tested in catalysis. The main results can be summarized as follows.

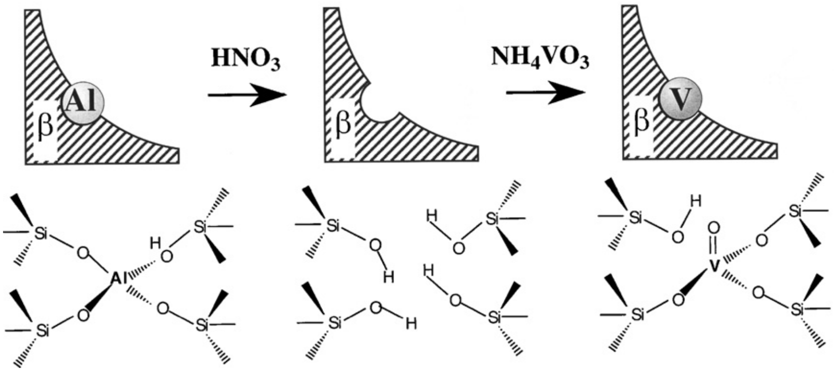

Fig. 4. Description of the 2-step post-synthesis method [28] and of the associated sites (see text).

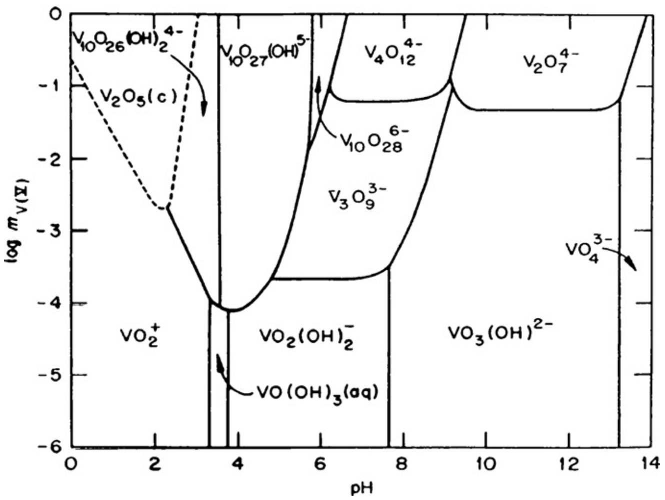

Fig. 5. Vanadium predominance diagram, according to Ref. [30] (see text).

5.1. First step: dealumination

(i) Chemical analysis shows that the Si/Al ratio changes from 11 for the parent AlBEA sample to over 1000 for sample SiBEA obtained after acid treatment, indicating the removal of aluminium.

(ii) X-ray diffractograms of AlBEA and SiBEA, i.e., before and after acid treatment, are similar (Fig. 6) [31], suggesting that the latter does not significantly affect the structure of the zeolite. While the determination of the unit cell parameters is made difficult because of the coexistence of several polytypes [27,32], it is nevertheless possible from the position of the diffraction peak (3 0 2) at $2\theta = 22–23^\circ$, within a given series of samples, to obtain information on the contraction/expansion of the framework [33]. The d_{302} spacing, calculated from the corresponding 2θ value, decreases from 3.96 (AlBEA) to 3.92 Å (SiBEA) suggesting a matrix contraction, consistent with the removal of aluminium [31].

(iii) Further evidence in favour of dealumination comes from IR experiments (results not shown) exhibiting the disappearance of IR bands at 3780, 3662 attributed to AlO–H and 3609 cm^{-1} to Al–O(H)–Si groups (bottom of Fig. 4) [31]. Meanwhile, narrow bands appear at 3736 and 3708 cm^{-1} which are related to isolated silanol groups together with a broad band at 3520 cm^{-1} due to H-bonded SiO–H groups in SiBEA (Fig. 7) [34], indicating the formation of vacant T-atom sites (T refers to tetrahedral Al and Si atoms of zeolites) associated with silanol groups (bottom of Fig. 4). NMR results (both ^{29}Si MAS NMR and $^{1}H–^{29}Si$ CP (cross polarization) MAS NMR) also are consistent with the formation of stable $^{29}Si–O^{1}H$ silanol groups [28].

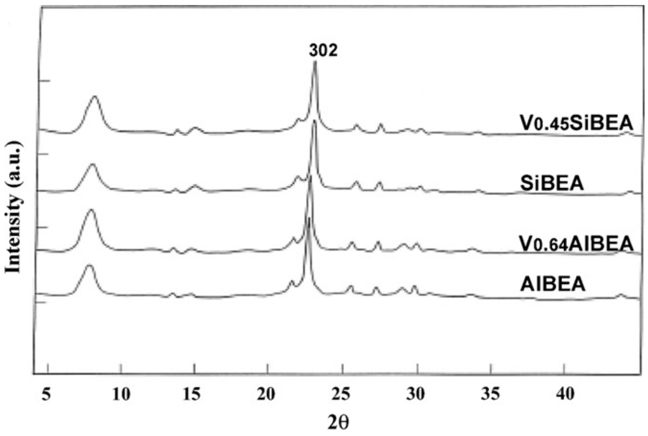

Fig. 6. X-ray diffractograms of AlBEA, $V_{0.64}AlBEA$, SiBEA and $V_{0.45}SiBEA$ samples [31] (see text).

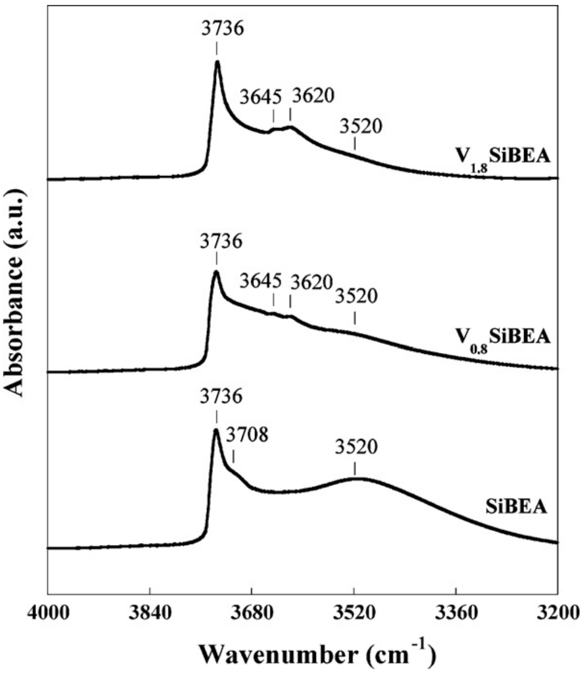

Fig. 7. FTIR spectra recorded at room temperature of SiBEA, $V_{0.8}SiBEA$ and $V_{1.8}SiBEA$ in the O–H stretching region after calcination of the samples at 773 K for 8 h in flowing oxygen followed by outgassing (10^{-3} Pa) at 573 K for 6 h [34]. The intensities of the IR spectra have been normalized with respect to the intensity of framework overtones located within the 2000–1800 cm−1 range (not shown) used as internal standards.

5.2. Second step: vanadium incorporation

(i) After contact of SiBEA samples with an aqueous NH_4VO_3 solution (pH = 2.5, room temperature, 3 days) and their recovery by centrifugation, chemical analysis shows that all the V atoms present in the initial solution are incorporated into the SiBEA framework up to a limit of 1.75 V atoms per unit cell [28,31]. This content is less than the amount of vacant T-atom sites generated by Al removal (5.3 per unit cell) but *ca.* 20 times higher the usually reported value for V-loaded zeolites prepared by hydrothermal synthesis [31].

(ii) While the incorporation of V does not affect the zeolite crystallinity, as evidenced by similar X-ray diffractograms of AlBEA, SiBEA and V_xSiBEA samples (Fig. 6) [31], it affects the d_{302} spacing which increases with V loading from 3.92 Å (SiBEA) up to a maximum value of 3.94 Å for a V/Si ratio of 0.021 [28]. Because of the relative values of the Al–O, Si–O and V–O bond lengths (1.790, 1.660 and 1.755 Å respectively) [28], this expansion of the lattice deduced from the d_{302} spacing strongly suggests that vanadium has been incorporated into the zeolite framework.

(iii) The vanadium of V_xSiBEA samples (up to *ca.* 1.75 V atoms per unit cell) is not removed by washing at room temperature either with water or an aqueous solution of ammonium acetate NH_4OAc, confirming that it has been incorporated into the BEA framework [31]. In sharp contrast, the vanadium added in similar conditions “on” AlBEA samples, i.e., on samples not previously dealuminated by acid treatment is readily removed by washing.

(iv) The incorporation of vanadium into SiBEA leads to a reduction of intensity of the IR bands of SiO–H groups, in particular at 3520 cm^{-1} (Fig. 7) suggesting that silanol groups react with the V precursor (bottom of Fig. 4) [28,31]. The vanadium is incorporated in SiBEA zeolite as isolated tetrahedral vanadium(V) species, with a non-hydroxylated pyramidal structure $(SiO)_3V{=}O$, with a V=O double bond and linked to the framework by V–OSi bonds (bottom of Fig. 4) [28,31]. This vanadium(V) species could interact with free Si–OH present in its vicinity as we have earlier reported [31]. Simultaneously, two small IR bands at 3620 and 3645 cm^{-1} appear (Fig. 7) which suggest that V_xSiBEA samples also contain V(V) sites with V(V)O–H groups with hydroxylated pyramidal structure $(SiO)_2(HO)V{=}O$. The intensity of these two bands increases with vanadium loading, particularly that at 3620 cm^{-1}. This suggests some heterogeneity of the vanadium sites in BEA zeolite, in line with two-dimensional ^{27}Al 3Q and 5Q MAS NMR measurements [34] allowing to distinguish two kinds of framework Al atom referred to as $Al_{Td}(2a)$ and $Al_{Td}(2b)$ in BEA zeolite.

On the basis of pyridine adsorption measurements, it has been concluded that the bands at 3620 and 3645 cm^{-1} correspond to V(V)O–H groups with Brønsted acidic character generated by the incorporation of vanadium into SiBEA zeolite [34].

(v) In order to get more insight into the environment of vanadium, the V_xSiBEA samples have been investigated by XANES and EXAFS (Fig. 8) [35]. The intense pre-edge peak in XANES spectra (Fig. 8A) due to the 1s–3d transition, mainly originating from admixture of oxygen 2p and vanadium 3d orbitals, indicates that vanadium is in a tetrahedral environment (same selection rules as for UV–vis spectroscopy). The pre-edge peak and the XANES spectra similar to those of the vanadyl tetrahedral $VO(O{-}iC_3H_7)_3$ compound [36] suggest the presence of one vanadyl V=O bond.

The tetrahedral environment of vanadium is confirmed by the single peak at *ca.* 1.6 Å (without phase-shift correction) observed in the Fourier transform of normalized k^3 weighted EXAFS spectra (Fig. 8B) [35]. The value of the coordination number calculated on the basis of the curve fitting analysis of the FT-EXAFS spectra is around 4 for all samples indicating that V is in a tetrahedral environment composed of four oxygen neighbours.

(vi) Diffuse reflectance (DR) UV–vis and EPR measurements have been performed to obtain information on the oxidation state of vanadium. The DR UV–vis spectrum of V_xSiBEA exhibits two main bands at 270 and 340 nm [28,31]. Because of the absence of d–d transition in the range 600–800 nm and of any V(IV) ($3d^1$) EPR signal, the two bands can only involve diamagnetic vanadium(V) ($3d^0$) ions and are assigned to $\pi(t_2) \rightarrow d(e)$ and to

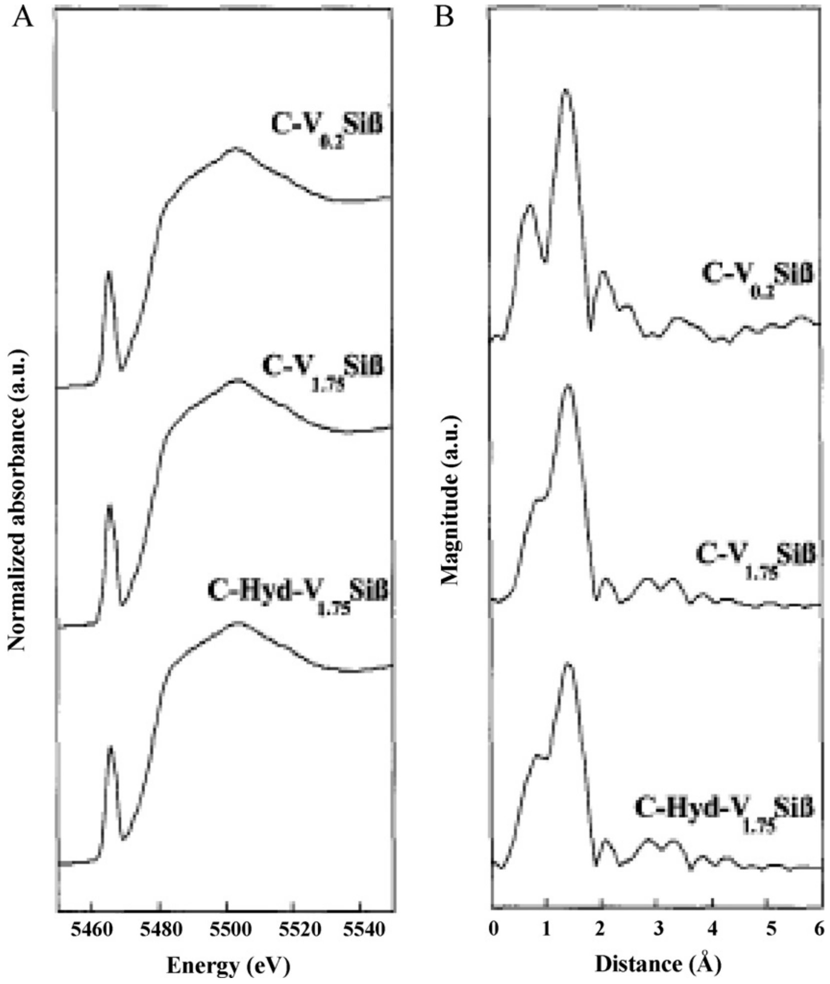

Fig. 8. XANES (A) and Fourier transforms of normalized k^3 weighted EXAFS (B) spectra at 295 K of C-$V_{0.2}$Siβ, C-$V_{1.75}$Siβ, and C-Hyd$V_{1.75}$Siβ outgassed at 473 K for 2 h (10^{-5} Torr), where C is calcination at 773 K (heating rate 50 K/h) in oxygen for 2 h and Hyd is hydration at 298 K in moist air for 30 h [35]. Also note that β and BEA are two notations referring to the same zeolite structure.

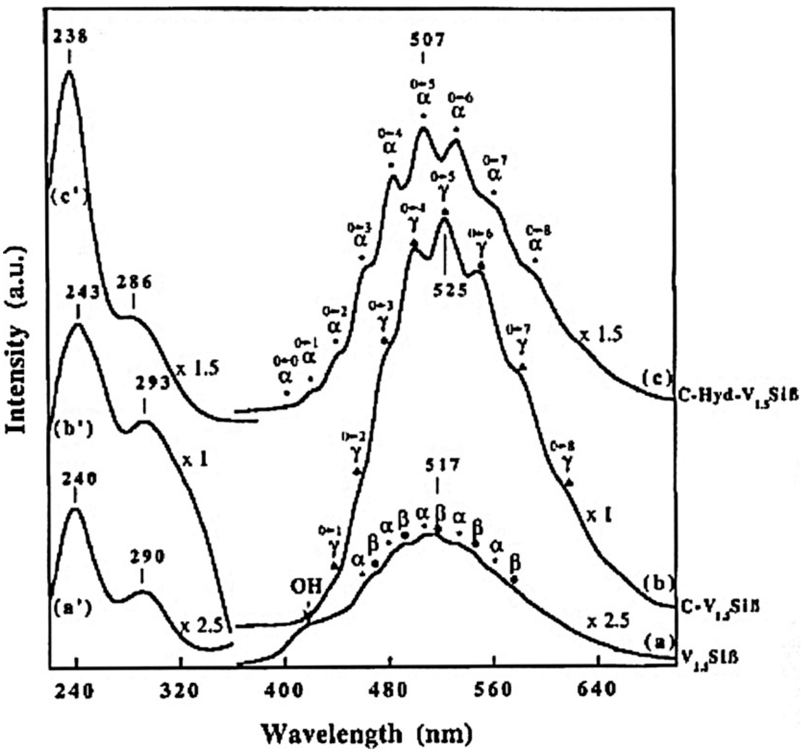

Fig. 9. Photoluminescence (a–c) and excitation (a′–c′) spectra recorded at 77 K of $V_{1.5}Si\beta$ outgassed at 353 K (10^{-3} Pa) (a, a′), of C-$V_{1.5}Si\beta$ outgassed at 473 K for 2 h (10^{-3} Pa) (b, b′), and C-Hyd$V_{1.5}Si\beta$ outgassed at 473 K for 2 h (10^{-3} Pa) (c, c′). C is calcination at 773 K (heating rate 50 K/h) in oxygen for 2 h and Hyd is hydration at 298 K in moist air for 30 h. Photoluminescence spectra were obtained under irradiation of 250 nm light. Excitation spectra were monitored at 520 nm [42]. Also note that β and BEA are two notations referring to the same zeolite structure.

$\pi(t_1) \rightarrow d(e)$ oxygen-tetrahedral V(V) charge transfer transitions, involving bridging (V–O–Si) and terminal (V=O) oxygen respectively, on the basis of work performed on V-silicalite [37].

(vii) Because of its sensitivity, photoluminescence spectroscopy has been at the origin of the so-called single molecule spectroscopy, aiming at following the behaviour of single molecules in very dilute systems [38]. This technique has been much employed in (photo)catalysis and adsorption studies because of its sensitivity and also its ability to detect vibrational fine structures [39,40]. Fig. 9 gives such an example for V_xSiBEA zeolites. The excitation (left part of Fig. 9) and emission (phosphorescence) (right part of Fig. 9) spectra are assigned to the following charge transfer (CT) process (Eq. (1)) [41,42]:

$$\underset{\text{singlet ground state}}{(V^{5+}{=}O^{2-})} \;\underset{\text{emission, h}\nu'}{\overset{\text{excitation, h}\nu}{\rightleftarrows}}\; \underset{\text{CT triplet excited state}}{\{V^{4+}{-}O^{-}\}^{*}} \qquad (1)$$

The emission which is observed at a lower frequency (ν') than that of the incident light (ν) (Eq. (1) and Fig. 9) occurs after some vibrational energy has been dissipated into the surroundings in a non-radiative way [39].

The charge transfer process of Eq. (1) illustrates the *redox* character of the V–BEA system. On this basis, the samples exhibit complex vibrational fine structures centred around 500–530 nm corresponding to transitions from the lowest vibrational level of the triplet excited state $T_1\{V^{4+}–O^-\}^*$ to the various vibrational levels of the singlet ground state $S_0(V^{5+}=O^{2-})$. The shape, position and intensity of the components of the vibrational fine structures depend on V content and pre-treatment of the samples as illustrated by Fig. 9. The important fact is that three vibrational fine structures can be distinguished which all correspond to distorted tetrahedral vanadium species, hereafter referred to as species α, β and γ, possessing one vanadyl V=O bond, with various degrees of distortion measured by the angle θ between the V=O and V–OSi(H) bonds of C_{3v} symmetry (Scheme 1) [41] varying in the series as follows:

$$\theta_\alpha(\text{C-HydV}_{1.5}\text{Si}\beta) < \theta_\gamma(\text{C-V}_{1.5}\text{Si}\beta) < \theta_\beta(\text{C-V}_{0.05}\text{Si}\beta).$$

Overall, the evidence is that the two-step post-synthesis method allows to obtain *redox* zeolites with *isolated* and *framework* vanadium. However, as pointed out above, IR, NMR as well as photoluminescence data evidence that those *isolated* and *framework* vanadium species are not *identical*. The problem becomes even more complex if the concentration of vanadium used in the second step is more important than the limit corresponding to 1.75 V atoms per unit cell quoted earlier (see Section 5.2, ii). As a matter of fact, above this threshold, the vanadium species in excess are found to be in extraframework position and thus in weaker interaction with the zeolite structure, explaining why they can be removed by washing [31].

5.3. Catalytic properties

Redox framework V_xSiBEA zeolites are active under UV–vis irradiation in the decomposition of NO in the presence of propane leading to high yield of N_2 [35]. The N_2 yield strongly depends on the distortion of tetrahedral V species which changes with calcination

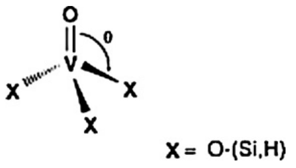

Scheme 1. Structure of the V(V) site in VSiBEA zeolite.

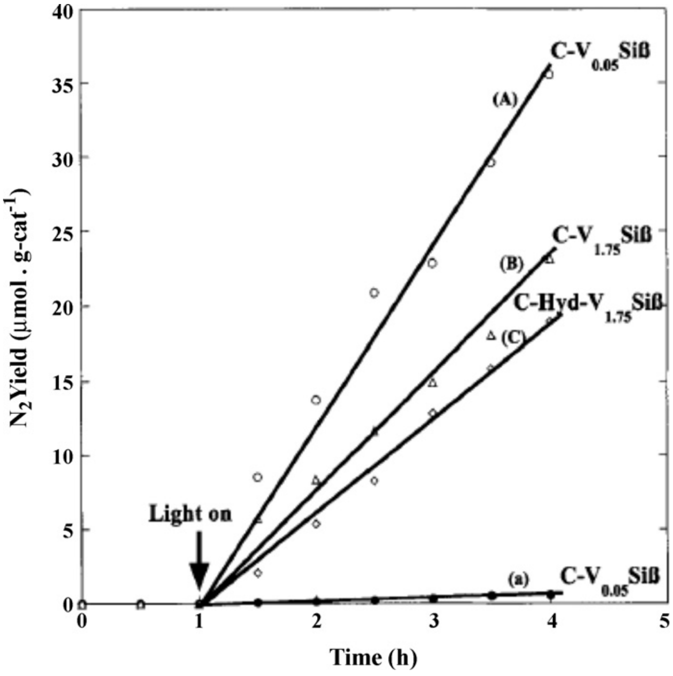

Fig. 10. Reaction time profile of the photocatalytic decomposition of NO at room temperature in the presence (10 Torr) (A, B and C) or absence (a) of propane on C-$V_{0.05}$Siβ (A, a) (mainly species β), C-$V_{1.75}$Siβ, (B) (mainly species γ), and C-Hyd$V_{1.75}$Siβ (C) (mainly species α) catalysts [35]. C is calcination at 773 K (heating rate 50 K/h) in oxygen for 2 h and Hyd is hydration at 298 K in moist air for 30 h. Also note that β and BEA are two notations referring to the same zeolite structure.

and hydration treatment of V_xSiBEA catalysts (Fig. 10) [35]. Both yield and distortion increase in the following order of the vanadium species:

$$\alpha \quad < \quad \gamma \quad < \quad \beta$$

The highest N_2 yield is found for the catalyst with tetrahedral V possessing the highest distortion, the lowest V=O bond length and the longest lifetime of its triplet excited state (Table 1) [35,41]. These data suggest that the very high activity of calcined $V_{0.05}$SiBEA catalyst in the photodecomposition of NO is related to the presence of isolated distorted tetrahedral V sites and to the efficient interaction of these V sites in their triplet excited state with NO, allowing to initiate its decomposition [35].

6. Application of the two-step post-synthesis method to other metal centres

The two-step post-synthesis method has been applied in its "aqueous" version (by reference to the NH_4VO_3 solution used in the second step) in order to incorporate into BEA other elements than vanadium, including Co(II) ($3d^7$) [43,44], Fe(III) ($3d^5$) [45–47], Cu(II) ($3d^9$) [48,49], and Cr(III) ($3d^3$) [50,51] and the catalytic properties of the resulting systems investigated, particularly in the selective reduction of NO by alcohols or propane [44–46,48,49] or the oxidative dehydrogenation of propane [51].

Table 1
Physicochemical parameters of tetracoordinated V species.

Type of tetracoordinated V species	α	γ	β
Vibrational energy (cm^{-1})	1018	1036	1054
V=O bond length (Å)	1.58	1.56	1.54
V–O single bonds lengths (Å)	1.72–180[a]		
O=V–O(Si,H) bond angle (labeled θ, Scheme 1)	θ_α	$\langle\theta_\gamma$	$\langle\theta_\beta$
Lifetime of the excited triplet states (ms)	28	49	88

[a] Data for reference compounds containing isolated VO_4 tetrahedra.

Although each element has its own characteristics, the molecular processes associated with each of the two steps of the method basically follow the sequence and description given above for vanadium (Sections 5.1 and 5.2).

There are however differences for some systems either because they behave in a specific way (case of Ni–SiBEA) or because the preparation method is not applied in its "aqueous" version (case of Nb–SiBEA, Ta–SiBEA and Ti–SiBEA).

6.1. Ni–SiBEA system [52]

Ni_xSiBEA zeolites have been prepared following the "aqueous" liquid route and using nickel nitrate as precursor for the second step of the post-synthesis method. In sharp contrast with the vanadium–BEA system, there is no expansion of the framework but rather a slight contraction upon contact of SiBEA with the nickel precursor solution, suggesting that nickel complexes such as $[Ni(H_2O)_6]^{2+}$ of O_h symmetry have not lead to the incorporation of nickel into zeolite framework. After calcination of the samples at 773 K in air for 3 h, XRD results show that now there is an expansion of the BEA structure, suggesting that Ni(II) ($3d^8$) ions have been incorporated. This is confirmed by diffuse reflectance UV–vis measurements which show that the incorporation is accompanied by a change from octahedral (O_h) to essentially tetrahedral (T_d) symmetry for the Ni(II) environment. XANES and EXAFS experiments at the Ni K edge, similar to those performed earlier for Ni/SiO_2 catalysts [53,54], are required to confirm this conclusion.

6.2. Nb–SiBEA [55,56] and Ta–SiBEA [57,58] systems

Here, we have used an "organic" liquid route in the second step of the post-synthesis method, which has the advantage to restrict the speciation of niobium and tantalum to a single type of mononuclear Nb(V) and Ta(V) (both d^0) species. There is another advantage that any possible dissolution of the oxide support, likely to occur at the water–oxide interface in the presence of ligands [59], can be largely avoided due to hydrophobic effects. Thus, an isopropanol solution of either niobium pentaethoxide $Nb(OC_2H_5)_5$ or tantalum pentaethoxide $Ta(OC_2H_5)_5$, both of D_{3h} symmetry, was put in contact with SiBEA obtained after the first dealumination step.

From the results obtained by XRD, NMR, IR, diffuse reflectance UV–vis and XPS, it is not surprising that the molecular processes associated with each of the two steps of the post-synthesis method globally follow the sequence and description given for vanadium, because both $Nb(OC_2H_5)_5$ and $Ta(OC_2H_5)_5$ also belong to group 5 elements with d^0 for the +V oxidation state. For both Nb–SiBEA and Ta–SiBEA systems, a heterogeneity of the sites has again been noted [55–58].

6.3. Ti–SiBEA system [60,61]

There are three noticeable advantages associated with the use of a gaseous precursor such as $TiCl_4$ ($3d^0$): (i) the speciation of titanium is restricted to the single species $TiCl_4$, (ii) there is no longer any need of a solvent, (iii) the precursor has the same tetrahedral symmetry as that of the site it should occupy after incorporation into the SiBEA structure.

The use of $TiCl_4$ vapor leads to significant amounts of Ti incorporated in SiBEA zeolite (5.8 wt.%), which have been characterized by an ensemble of techniques (XRD, IR, NMR, diffuse reflectance UV–vis, XPS). In line with the results described for other d^0 systems, the molecular processes associated with each of the two steps of the post-synthesis method globally follow the sequence and description given for vanadium.

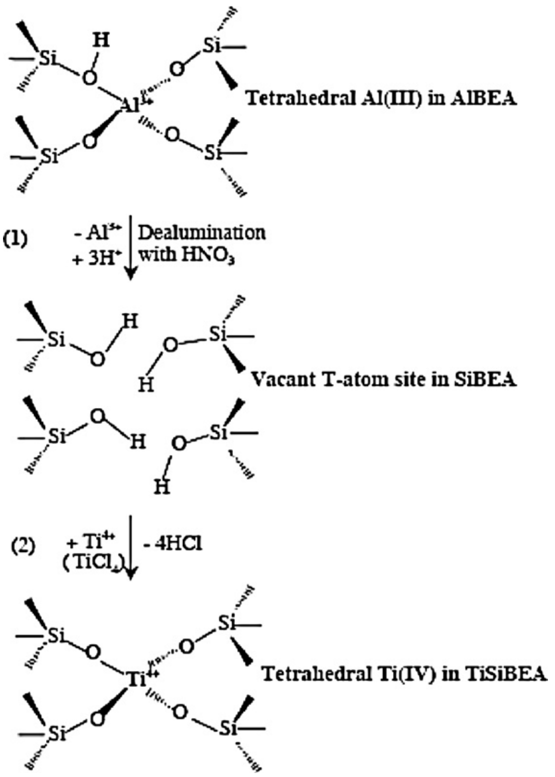

Scheme 2. Possible pathway of formation of tetrahedral Ti(IV) in TiSiBEA zeolite.

An important difference though with respect to vanadium is the symmetry of the site occupied by titanium in SiBEA which appears to be less distorted (compare Scheme 1 for vanadium [41] and Scheme 2 for titanium [60]). This is probably due to the nature of the precursor. It would be most interesting to confirm whether the latter can influence the final structure of the element incorporated into the BEA zeolite. Along this idea, it would be useful to prepare V_xSiBEA zeolites from gas phase precursors such as VCl_4 (T_d symmetry) and $VOCl_3$ (C_{3v} symmetry), as investigated earlier with silica [62], or similarly $TiCl_4$ (T_d symmetry) and $TiOCl_2$ (C_{2v} symmetry). This raises the question of memory effect in catalyst preparation, a point considered earlier from the coordination viewpoint [63].

Finally, as in the previous cases, Ti–SiBEA also exhibits a heterogeneity of the metal sites [60].

7. Discussion: *pro et contra*

The results described above suggest that the preparation of redox zeolite catalysts with isolated and framework metal centres has been successfully achieved by means of the two-step post-synthesis method and whatever the route (aqueous solution, organic liquid or gas phase) used in the second step. Because the preparation steps are performed at room temperature and atmospheric pressure, i.e., those of the so-called chimie douce, their implementation is less energy demanding than other methods requiring more drastic conditions. This may constitute an appreciable advantage.

On the basis of data obtained at the macroscopic and molecular levels by chemical analysis and physical techniques, it is shown that the first step of the method, i.e., the treatment of the zeolite by an acid solution, is associated with the removal of aluminium atoms from the BEA framework manifested by disappearance of the corresponding AlO–H groups, with simultaneous formation of T-atom vacant sites with associated SiO–H groups. The second step, i.e., contact of the resulting dealuminated solid with the molecular precursor, is linked to the incorporation of the metal centre M into the zeolite. The cases M = V(V), Nb(V), Ta(V) and Ti(IV) (all d^0 ions) were discussed above in some detail and the others (M = Co(II) ($3d^7$), Fe(III) ($3d^5$), Cu(II) ($3d^9$), and Cr(III) ($3d^3$)) just quoted.

The only notable exception to this general trend is the case of Ni(II) ($3d^8$) where the nickel atoms are not directly incorporated into the zeolite framework during the second step. A calcination step is required to achieve this target. The origin of this exception is not known as yet. Several factors may be considered, including crystal fields effects (absent in the case of d^0 and d^5 ions but present in the others), geometric constraints (relative sizes of the vacant site obtained after dealumination and of the ion to be incorporated), and change of symmetry between the molecular metal precursor (e.g., $[Ni(H_2O)_6]^{2+}$, $Nb(OC_2H_5)_5$, or $TiCl_4$) and the final state after incorporation of the metal centre into the SiBEA zeolite.

There is still some way to go before obtaining *single site* catalysts, where all the metal centres are all *identical*. As a matter of fact, a heterogeneity of the sites has been noted repeatedly for the systems V-, Ni-, Nb–, Ta– and Ti–SiBEA zeolites discussed above as well as those investigated earlier (Section 6), even though efforts have been made to vary the nature (water/organic liquid solvent, gas phase) and symmetry of the molecular metal precursor, as well as the oxidation and electronic structure of the metal centre. This heterogeneity most probably originates from the nature of BEA zeolite and the coexistence of several polytypes [27,32].

Obviously, to avoid this problem, it would be interesting to apply the two-step post-synthesis method to zeolites such as ZSM-5 (MFI) and, following Haag et al. [20], to investigate a much larger range of metal content.

ZSM-5 (MFI) zeolite exhibits substantial chemical uniformity of sites [20], which does not rule out topologically different locations in the ZSM-5 framework, with characteristic distances beyond the range of localized chemical forces. The problem of crystallographic sites has been investigated earlier, in particular by ^{29}Si (with nuclear spin $I = ½$) MAS NMR with unprecedented resolution, in the case of highly siliceous zeolites, KZ-2, ZSM-12, BEA [64] and ZSM-5 [65]. This is of course more difficult to achieve with ^{27}Al ($I = 5/2$) because of quadrupolar effects. These considerations raise the question as to which chemical and/or topological uniformity of the catalytically active sites the reactants are sensitive.

Model oxide systems such as those based on zeolites or polyoxometallates [66–70] are very attractive matrices for they have their own catalytic properties but also because their structure can be characterized topologically by structure-sensitive techniques such as XRD, locally by element-specific spectroscopies such as

Fig. 11. Lunch at the top of the Université Pierre et Marie Curie tower, Paris, just before the Doctor Honoris Causa (DHC) ceremony (from left to right: Prof. Jerzy Haber, Michel Che and Mrs Hanka Haber) on November 23rd 1994.

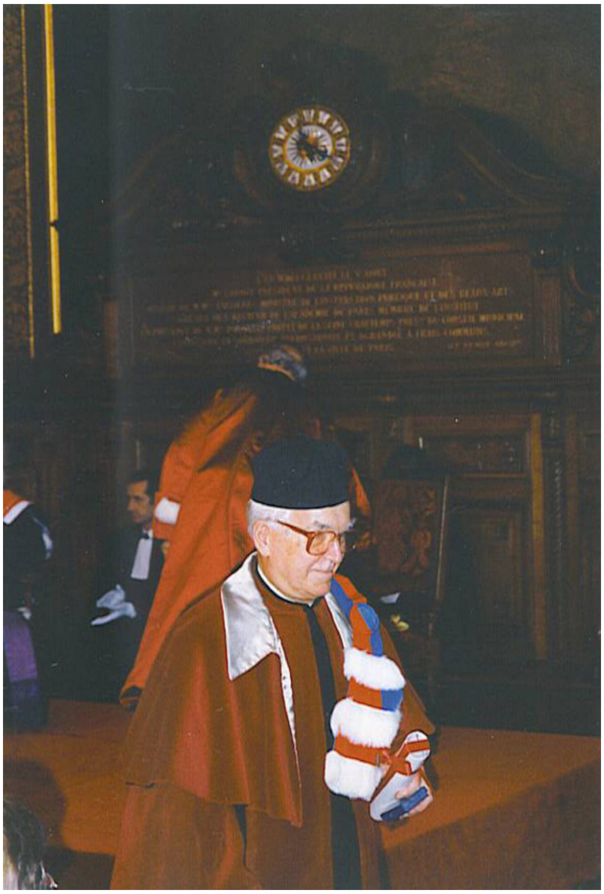

Fig. 12. Professor Jerzy Haber during the DHC ceremony in the Grand Salon d'Honneur of La Sorbonne, Paris, on the afternoon of November 23rd 1994.

MAS NMR and chemically by site-sensitive reactions such as those involved in catalysis. Investigations based on such model oxides as well as theoretical calculations [71,72] are likely to improve our understanding of single site catalysts, which are currently the subject of very intense research [73–77].

The Cracow school was among the pioneers of this experimental-theoretical approach to oxide-catalyzed reactions [78] highly appreciated world-wide. For his major contribution to catalysis, Prof. J Haber was awarded the Doctor Honoris Causa degree by our University on the 23rd November 1994 (Figs. 11 and 12). The Institute of Catalysis and Surface Chemistry (PAN) is a living testimony of his leadership. We all are grateful to Mrs. Hanna Haber for having greatly contributed to this success.

8. Conclusions

This contribution gives the definition of homogeneous single site catalysts before considering the speciation problems associated with the preparation of their heterogeneous analogs. Following Haber's interest for vanadium oxide catalysts, it describes a two-step post-synthesis method to prepare redox framework single site zeolites and its application to obtain V_xSiBEA catalysts. The molecular processes relevant to each of the two steps of the method are described on the basis of data obtained with techniques employed at the macroscopic and molecular levels. The two-step post-synthesis method in its original "aqueous" version or slightly modified (organic liquid route or gas phase route) has been used to prepare zeolite catalysts with other elements, including nickel, niobium, tantalum and titanium. The advantages and disadvantages of the two-step post-synthesis method are discussed and possible ways to obtain/investigate *redox framework single site* zeolite catalysts with *identical* sites are suggested.

Acknowledgement

S.D. gratefully acknowledges the CNRS (France) for financial support as Assistant Researcher.

References

[1] J. Haber, Catal. Today 142 (2009) 100.
[2] S. Dzwigaj, J. Haber, T. Romotowski, Zeolites 3 (1983) 134.
[3] S. Dzwigaj, J. Haber, T. Romotowski, Zeolites 4 (1984) 147.
[4] M. Derewinski, S. Dzwigaj, J. Haber, Zeolites 4 (1984) 214.
[5] M. Derewinski, J. Haber, J. Ptaszynski, V.P. Shiralkar, S. Dzwigaj, Stud. Surf. Sci. Catal. 18 (1984) 209.
[6] M. Derewinski, S. Dzwigaj, J. Haber, Stud. Surf. Sci. Catal. 24 (1985) 639.
[7] V.A. Matyshak, M.M. Slin'ko, R.A. Gazarov, O.V. Krylov, S. Dzwigaj, J. Haber, Kinet. Katal. 30 (1989) 155.
[8] M. Derewinski, S. Dzwigaj, J. Haber, R. Mostowicz, B. Sulikowski, Zeit. Phys. Chem. 171 (1991) 53.
[9] M. Derewinski, S. Dzwigaj, J. Haber, Pol. J. Chem. 66 (1991) 545.
[10] K. Bruckman, J.M. Tatibouet, M. Che, E. Serwicka, J. Haber, J. Catal. 139 (1993) 455.
[11] K. Bruckman, M. Che, J. Haber, J.M. Tatibouet, Catal. Lett. 25 (1994) 225.
[12] J.M. Tatibouet, C. Montalescot, K. Bruckman, J. Haber, M. Che, J. Catal. 169 (1997) 22.
[13] G. Vavon, A. Husson, Comptes Rendus 175 (1922) 277.
[14] H.S. Taylor, Proc. R. Soc. Lond. A 108 (1925) 105.
[15] M. Boudart, J. Mol. Catal. A 120 (1997) 271.
[16] A. Andersen, H.G. Cordes, J. Herwig, W. Kaminsky, A. Merk, R. Rottweiler, J. Pein, H. Sinn, H.J. Vollmer, Angew. Chem. Int. Ed. Engl. 15 (1976) 630.
[17] H. Sinn, W. Kaminsky, Adv. Organomet. Chem. 18 (1980) 99.
[18] G.W. Coates, Chem. Rev. 100 (2000) 1223.
[19] G.G. Hlatky, Chem. Rev. 100 (2000) 1347.
[20] W.O. Haag, R.M. Lago, P.B. Weisz, Nature 309 (1984) 589.
[21] D.M. Templeton, F. Ariese, R. Cornelis, L.G. Danielsson, H. Muntau, H.P. van Leeuwen, R. Lobinski, Pure Appl. Chem. 72 (2000) 1453.
[22] V. Moulin, C. Moulin, Radiochim. Acta 89 (2001) 773.
[23] M. Che, A.J. Tench, Adv. Catal. 32 (1983) 1.
[24] M. Che, A.J. Tench, Adv. Catal. 31 (1982) 77 (first published as AERE, Report – R 9971 Nov. 1980).
[25] J.M. Thomas, J. Klinowski, S. Ramadas, M.W. Anderson, C.A. Fyfe, G.C. Gobbi, Am. Chem. Soc. Symp. Ser. 218 (1983) 159.
[26] R.L. Wadlinger, G.T. Kerr, E.J. Rosinski, US Patent 3,308,069 (1967).
[27] J.B. Higgins, R.B. LaPierre, J.L. Schlenker, A.C. Rohrman, J.D. Wood, G.T. Kerr, W.J. Rohrbaugh, Zeolites 8 (1988) 446.
[28] S. Dzwigaj, M.J. Peltre, P. Massiani, A. Davidson, M. Che, T. Sen, S. Sivasanker, Chem. Commun. (1998) 87.
[29] E. Bourgeat-Lami, F. Fajula, D. Anglerot, T. des Courieres, Micropor. Mater. 1 (1993) 237.
[30] C.F. Baes Jr., R.E. Mesmer, The Hydrolysis of Cations, Wiley, New York, 1976, p. 210.
[31] S. Dzwigaj, P. Massiani, A. Davidson, M. Che, J. Mol. Catal. 155 (2000) 169.
[32] (a) J.M. Newsam, M.M.J. Treacy, W.T. Koetsier, C.B. Degruyter, Proc. R. Soc. Lond. A 420 (1988) 375;
(b) M.M.J. Treacy, J.M. Newsam, Nature 332 (1988) 249.
[33] M.A. Camblor, A. Corma, J. Pérez-Pariente, Zeolites 13 (1993) 82.
[34] R. Hajjar, Y. Millot, P.P. Man, M. Che, S. Dzwigaj, J. Phys. Chem. C 112 (2008) 20167.
[35] S. Dzwigaj, M. Matsuoka, M. Anpo, M. Che, Res. Chem. Intermed. 29 (2003) 665.
[36] S. Higashimoto, M. Matsuoka, S.G. Zhang, H. Yamashita, O. Kitao, H. Hidaka, M. Anpo, Micropor. Mesopor. Mater. 48 (2001) 329.
[37] G. Centi, S. Perathoner, F. Trifiro, A. Aboukais, C.F. Aïssi, M. Guelton, J. Phys. Chem. 65 (1992) 518.
[38] (a) W.E. Moerner, L. Kador, Phys. Rev. Lett. 62 (1989) 2535;
(b) M. Orrit, J. Bernard, Phys. Rev. Lett. 65 (1990) 2716;
(c) C. Bräuchle, D.C. Lamb, J. Michaelis (Eds.), Single particle tracking and single molecule energy transfer, Wiley-VCH, Weinheim, 2010.
[39] M. Anpo, M. Che, Adv. Catal. 44 (1999) 119.
[40] M. Anpo, S. Dzwigaj, M. Che, Adv. Catal. 52 (2009) 1.
[41] S. Dzwigaj, M. Matsuoka, R. Franck, M. Anpo, M. Che, J. Phys. Chem. B 102 (1998) 6309.
[42] S. Dzwigaj, M. Matsuoka, M. Anpo, M. Che, J. Phys. Chem. B 104 (2000) 6012.
[43] S. Dzwigaj, M. Che, J. Phys. Chem. B 110 (2006) 12490.
[44] J. Janas, T. Machej, J. Gurgul, R.P. Socha, M. Che, S. Dzwigaj, Appl. Catal. B 75 (2007) 239.
[45] S. Dzwigaj, J. Janas, T. Machej, M. Che, Catal. Today 119 (2007) 133.
[46] J. Janas, J. Gurgul, R.P. Socha, T. Shishido, M. Che, S. Dzwigaj, Appl. Catal. B 91 (2009) 113.
[47] K. Hadjiivanov, E. Ivanova, R. Kefirov, J. Janusz, A. Plesniar, S. Dzwigaj, M. Che, Micropor. Mesopor. Mater. 131 (2010) 1.

[48] S. Dzwigaj, J. Janas, J. Mizera, J. Gurgul, R.P. Socha, M. Che, Catal. Lett. 126 (2008) 36.
[49] S. Dzwigaj, J. Janas, J. Gurgul, R.P. Socha, T. Shishido, M. Che, Appl. Catal. B 85 (2009) 131.
[50] K. Hadjiivanov, A. Penkova, R. Kefirov, S. Dzwigaj, M. Che, Micropor. Mesopor. Mater. 124 (2009) 59.
[51] J. Janas, J. Gurgul, R.P. Socha, J. Kowalska, K. Nowinska, T. Shishido, M. Che, S. Dzwigaj, J. Phys. Chem. C 113 (2009) 13273.
[52] D. Li, F. Averseng, S. Dzwigaj, M. Che, (2011) in press.
[53] J.Y. Carriat, M. Che, M. Kermarec, M. Verdaguer, A. Michalowicz, J. Am. Chem. Soc. 120 (1998) 2059.
[54] O. Clause, L. Bonneviot, M. Che, H. Dexpert, J. Catal. 130 (1991) 21.
[55] S. Dzwigaj, Y. Millot, C. Méthivier, M. Che, Micropor. Mesopor. Mater. 130 (2010) 162.
[56] F. Tielens, T. Shishido, S. Dzwigaj, J. Phys. Chem. C 114 (2010) 3140.
[57] S. Dzwigaj, Y. Millot, M. Che, Catal. Lett. 135 (2010) 169.
[58] F. Tielens, T. Shishido, S. Dzwigaj, J. Phys. Chem. C 114 (2010) 9923.
[59] X. Carrier, J.F. Lambert, M. Che, J. Am. Chem. Soc. 119 (1997) 10137.
[60] J.P. Nogier, Y. Millot, P.P. Man, T. Shishido, M. Che, S. Dzwigaj, J. Phys. Chem. 113 (2009) 4885.
[61] J.P. Nogier, Y. Millot, P.P. Man, C. Methivier, M. Che, S. Dzwigaj, Catal. Lett. 130 (2009) 588.
[62] M. Anpo, M. Sunamoto, M. Che, J. Phys. Chem. 93 (1989) 1187.
[63] (a) M. Che, L. Bonneviot, Pure Appl. Chem. 60 (1988) 1369;
(b) J.F. Lambert, M. Che, J. Mol. Catal. A 162 (2000) 5.
[64] C.A. Fyfe, H. Strobl, G.T. Kokotailo, C.T. Pasztor, G.E. Barlow, S. Bradley, Zeolites 8 (1988) 132.
[65] C.A. Fyfe, J.H. O'Brien, H. Strobl, Nature 326 (1987) 281.
[66] P. Gouzerh, M. Che, Actual. Chim. 298 (2006) 9.
[67] M. Fournier, C. Louis, M. Che, P. Chaquin, D. Masure, J. Catal. 119 (1989) 400.
[68] S. Dzwigaj, M. Che, B. Grzybowska, I. Gressel, K. Samson, Stud. Surf. Sci. Catal. 172 (2007) 385.
[69] S. Dzwigaj, I. Gressel, B. Grzybowska, K. Samson, Catal. Today 114 (2006) 237.
[70] K. Bruckman, B. Grzybowska, M. Che, J.M. Tatibouet, Appl. Catal. 96 (1993) 279.
[71] F. Tielens, M. Calatayud, S. Dzwigaj, M. Che, Micropor. Mesopor. Mater. 119 (2009) 137.
[72] D. Masure, P. Chaquin, C. Louis, M. Che, M. Fournier, J. Catal. 119 (1989) 415.
[73] J.M. Thomas, R. Raja, D.W. Lewis, Angew. Chem. Int. Ed. 44 (2005) 6456.
[74] J.M. Thomas, R. Raja, Top. Catal. 40 (2006) 3.
[75] H. Yamashita, K. Mori, S. Shironita, Y. Horiuchi, Catal. Surv. Asia 12 (2008) 88.
[76] A.J. Ward, A.F. Masters, T. Maschmeyer, in: J.-M. Basset, R. Psaro, D. Roberto, R. Ugo (Eds.), Recent Advances in Surface Organometallic Chemistry, Wiley-VCH, Weinheim, 2009, p. 167.
[77] J.M. Thomas, R. Raja, Top. Catal. 53 (2010) 848.
[78] J. Haber, M. Witko, R. Tokarz, Appl. Catal. A 157 (1997) 3.